CO-PYROLYSIS OF COAL AND OIL SHALE I: THERMODYNAMICS AND KINETICS OF HYDROGEN SULFIDE CAPTURE BY OIL SHALE

L. Johnson, M. Rostam-Abadi, I. Mirza, M. Stephenson, and C. Kruse

Illinois State Geological Survey
Champaign, Illinois 61820

Introduction

The potential for producing crude oil and a compliance char (less than 1.2 lb SO_2/ MMBtu) by pyrolysis of Illinois Basin high volatile bituminous coals has been recognized for years but it has not been realized mainly because these coals agglomerate when pyrolyzed and because the chars have a relatively high sulfur content. The feasibility of using oil shale during pyrolysis of high sulfur coals and hydrodesulfurization of the resultant coal char is currently being investigated at the Illinois State Geological Survey (ISGS). Although still in the early stages of process development, three processes have been conceived which use oil shale with coal. In the first process, coal and oil shale, or coal and retorted shale are pyrolyzed in a fluidized bed reactor(FBR). In the second process, spent oil shale and coal are processed in a FBR. In the third process, coal and oil shale are pyrolyzed in a multistaged FBR with coal and oil shale occupying separate, alternating stages. The coal char product from these processes must be hydrodesulfurized to produce a compliance char.

Pyrolyzing coal and oil shale together could have many advantages over the pyrolysis of either material separately. First, preliminary ISGS data indicates that the inert minerals in oil shale dilute the coal-shale mixture, reducing the agglomeration of caking coals. Secondly, liquid and gaseous hydrocarbons are produced from both coal and oil shale. Thirdly, the carbonate minerals found in oil shale (calcite, dolomite) and their corresponding oxides formed during pyrolysis can act as scavengers of hydrogen sulfide during pyrolysis and hydrodesulfurization. Research efforts have recently been initiated at ISGS to obtain engineering data in the above areas. The results presented are the first phase of a larger thermodynamics and kinetics study of the reactions between oil shale and H_2S. The findings of this initial literature review provide the basis for the second phase of our research which will be presented in future publications.

Decomposition Reactions

The most significant reactions of carbonate minerals which occur during the co-pyrolysis of coal and oil shale are shown in table 1. The extent and pathway of carbonate decomposition are significant because they determine which sorbent(s) are present during hydrodesulfurization or pyrolysis. The overall thermal efficiency of the process and the physical properties of the product oxide are also affected by the extent of carbonate decomposition.

Calcium carbonate in oil shale is found as calcite and dolomite. Dolomite ($CaCO_3MgCO_3$) is a single phase of calcium and magnesium carbonate with its own unique crystal structure. During decarbonation of the magnesium component to form half-calcined dolomite, $CaCO_3MgO$, (hc-dolomite) small crystallites of MgO appear indicating a separation of the calcium and magnesium phases. This separation continues through the second decarbonation to form fully-calcined dolomite, CaOMgO, (fc-dolomite). Based on this observation, one would predict that the behavior of the solid more closely resembles an intimate mixture of its calcium and magnesium components as the calcination proceeds from dolomite to fc-dolomite.

Table 1. Shale Mineral Reactions Occurring During Pyrolysis and Hydrodesulfurization

Equation	H_{298} (Kcal/mole)	Equation No
Decomposition Reactions		
$CaCO_3 \rightarrow CaO + CO_2$	43	1)
$MgCO_3 \rightarrow MgO + CO_2$	28	2)
$CaCO_3MgCO_3 \rightarrow (CaCO_3 + MgO) + CO_2$	30	3)
$CaCO_3MgCO_3 \rightarrow (CaO + MgO) + 2CO_2$	73	4)
Desulfurization Reactions		
$CaCO_3 + H_2S \rightarrow CaS + CO_2 + H_2O$	28	5)
$CaO + H_2S \rightarrow CaS + H_2O$	-15	6)
$CaCO_3MgO + H_2S \rightarrow (CaS + MgO) + H_2O + CO_2$	28	7)
$CaOMgO + H_2S \rightarrow (CaS + MgO) + H_2O$	-15	8)
$CaCO_3MgCO_3 + H_2S \rightarrow (CaS + MgO) + 2CO_2 + H_2O$	62	9)

Both the extent and mechanism of dolomite decomposition are affected by the partial pressure of CO_2. Haul and Markus (1952) followed the decomposition of dolomite by thermogravimetric analysis of powdered dolomite at 500-900°C under various partial pressures of CO_2. Their results, shown in figure 1, indicate that the decomposition occurs by two different pathways:

$$CaCO_3MgCO_3 \rightarrow [CaCO_3 + MgO] + CO_2 \rightarrow [CaO + MgO] + 2CO_2 \qquad \text{Path A}$$

$$CaCO_3MgCO_3 \rightarrow [CaO + MgO] + 2CO_2 \qquad \text{Path B}$$

The decomposition followed Path A when the partial pressure of CO_2 was 12-24 mmHg while Path B prevails at higher CO_2 pressures. Since the equilibrium constant for the decomposition reaction is simply the partial pressure of CO_2, the concentration of CO_2 affects both the mechanism and extent of decomposition. For processes in which a carbonaceous material (retorted shale or coal char) is oxidized to supply energy for the pyrolysis stage, the presence of CO_2 in the recycled combustion gases will inhibit the carbonate decomposition.

The onset of decomposition is affected by the presence of steam. MacIntire and Stansell (1953) report that calcium and magnesium components of dolomite decompose about 200°C lower than when air is used alone. The same effect was observed by Burnham et al. (1980) except dolomite was affected to a much greater extent than calcite.

Decomposition reactions are highly endothermic, thus they adversely affect the thermal efficiency of the process. Boynton (1980) described the heat balance for the calcination of limestone in a rotary kiln. Between 1.7 and 4.8 MMBtu/ton of $CaCO_3$ are expended depending on the heat recovery systems employed. The minimum heat for calcination at the dissociation temperature is 2.5 MMBtu/ton of calcite or 0.61 MMBtu/ton of shale to calcine an average western shale containing 33% carbonates. Chen et al. (1982) used the ASPEN computer simulation system to study the effect of calcite decomposition on the overall thermal efficiency of an oil shale retort.

Finally, the rate and the temperature of decomposition affect the pore structure of the carbonate mineral particles as well as the shale. Steen et al. (1980) reported an increase in porosity from 12 to 29% accompanied by an increase in surface area from 0.3 to 8.9 m^2/g after half calcination of a dolomite sample. Surface area and porosity have a strong influence on the rate of sulfidation and absorbance capacity of the minerals.

Campbell (1978) and McCarthy et al. (1984) have shown that the under typical retorting conditions $CaCO_3$ also reacts with SiO_2. The competing reactions are:

$$xCaCO_3 + ySiO_2 \rightarrow Ca_xSi_yO_{x+2y} + xCO_2$$

$$CaCO_3 \rightleftharpoons CaO + CO_2$$

When a high CO_2 partial pressure and a slow heating rate were used, the carbonate reaction to form silicates increased because of the greater length of time required to reach the decarbonation temperature. Decomposition to CaO is very rapid once this temperature is reached. Oxide formation occurs at 600 to 750°C depending on the CO_2 partial pressure whereas silicate formation occurs at about 700-800°C. Therefore, this undesirable depletion of available carbonates would not be significant during pyrolysis (600°C) but may become a problem during hydrodesulfurization (750-850°C) or if the shale is retorted prior to mixing with the coal to be pyrolyzed.

Thermodynamics of Desulfurization Reactions

The ISGS application of the minerals in oil shale differs markedly from fuel gas desulfurization by carbonates. During pyrolysis and hydrodesulfurization, H_2O, H_2, CO, CO_2 and H_2S influence the H_2S adsorption equilibria, i.e. equations 5-9, table 1. Optimal temperatures, pressures, flowrates, etc. have been specified for pyrolysis and hydrodesulfurization processes, but these conditions may not be the most favorable for H_2S adsorption. In the following discussion the thermodynamics of H_2S adsorption by oil shale minerals are reviewed while taking into consideration the limited range of operating conditions typical of pyrolysis and hydrodesulfurization processes.

The reaction between calcium oxide and hydrogen sulfide (eqs. 6 and 8) has been studied by many researchers (Uno, 1951; Rosenquist, 1951; Curran et al., 1967). Pell (1971) summarized these experimental studies with the following least squares fit of their data:

$$\log K = \log \frac{P_{H_2O}}{P_{H_2S}} = 3519.2/T - 0.268 \qquad 10)$$

Pell combined this expression with the data given by Hill and Winter (1956) for the decomposition of calcium carbonate to find the following equilibrium expression for the reaction between hc-dolomite and hydrogen sulfide (eq. 7):

$$\log K = \log \frac{P_{H_2O} \cdot P_{CO_2}}{P_{H_2S}} = 7.253 - 5280.5/T \qquad 11)$$

Combining equation 11 with the data given by Stern and Weise (1969) on the decomposition of magnesium carbonate, the following expression for the equilibrium between dolomite and H_2S (eq. 9) is obtained:

$$\log K = \log \frac{(P_{CO_2})^2 \cdot P_{H_2O}}{P_{H_2S}} = 16.19 - 10{,}553/T \qquad 12)$$

Plots of log K vs 1/T derived from equations 10-12 are shown in figures 2 and 3. Plots from thermodynamic calculations based on the data of Barin et al. (1977) and Mills (1974) are also shown. A number of interesting observations can be made from these figures.

1. The efficiency of calcium oxide as an H_2S absorbent decreases at higher temperatures whereas the efficiency of calcium carbonate increases.

2. The thermodynamic calculations of the equilibrium constant for the reaction of H_2S and lime agree well with the experimental data. Since only thermodynamic data for dolomite exists, the calculations for the sulfidation of the full and half calcines were made as shown above, i.e., starting with dolomite calculations and combining them with decomposition data. Therefore, the good match between the thermodynamic and experimental values shown in figure 3 reflect accurate predictions of the extent of carbonate decomposition, not sulfidation.

3. As was mentioned earlier, the behavior of fc-dolomite is nearly the same as that of calcium oxide, and the reaction of hc-dolomite with hydrogen sulfide is similar to that of calcite. On the other hand, dolomite behaves completely different than calcite.

When coal is pyrolyzed, pyrite (FeS_2) is converted to pyrrhotite (FeS) and hydrogen sulfide. The hydrogen sulfide may then be removed with the off-gas or be captured in the carbon matrix of the coal or char (Huang and Pulsifer, 1977). Many studies of the reaction of H_2S with char, commonly referred to as the back-reaction, have been carried out (Robinson, 1976; Zielke et al., 1954; Jones et al., 1966). Depending on the temperature and nature of the char, the back reaction can occur at H_2S concentrations as low as 300 ppm. An acceptable scavanger should limit the H_2S concentration to this level to inhibit the back-reaction. Figure 4 shows that under typical pyrolysis conditions, calcium minerals are capable of maintaining this level if equilibrium is reached. The desired equilibrium partial pressure, i.e., below 300 ppm, is predicted at all temperatures of interest when CaO is present, at temperatures above 400°C when dolomite is present, and at temperatures above 750°C when $CaCO_3$ is present. Data from the Lurgi-Rhurgas oil shale distillation process which recycles oxidized shale to the pyrolysis bed demonstrates the reactivity of CaO toward H_2S. At a recycle ratio of about 7/1 and at 650°C, hydrogen sulfide concentrations of ~1300 ppm and ~4000 ppm in the off gas have been reported by Schmalfeld (1975) and Weiss (1982), respectively. Sitrai (1984) has also shown that retorting a 1:1 mixture of oil shale and shale ash reduces the concentration of H_2S in the off-gas to less than 100 ppm.

The decomposition and desulfurization reactions of carbonates occur in parallel. Therefore, the competition between the two reactions should be considered. The FACT thermodynamics computing system (Bale et al., 1979) was used to develop the phase stability diagrams for Mg-C-H-O-S and the Ca-C-H-O-S systems shown in figures 5-7. Magnesium carbonate is unstable with respect to the oxide at 327°C and .10 atm. CO_2. As shown in figure 5, at hydrogen sulfide concentrations of 0.6% or higher, sulfidation is inhibited until about 1227°C. This result agrees with Westmoreland and Harrison (1980) who concluded that MgO is too stable to be used as an H_2S acceptor.

Phase diagrams for the Ca-O-H-S-C system at about 500°C, the maximum pyrolysis temperature, and 750°C, a typical hydrodesulfurization temperature for coal char, are shown in figures 6 and 7. At 600°C calcium oxide exists only at carbon dioxide

pressures lower than about 0.01 atm. Calcium oxide will react with H_2S at gas concentrations as low as 10 ppm whereas, depending on the CO_2 concentration, H_2S concentrations from 100 to 1000 ppm are required before the carbonate will undergo sulfidation. At 750°C the reactivity of the oxide is nearly unchanged. However, at this temperature $CaCO_3$ decomposes at CO_2 pressures as high as 0.2 atm and will undergo sulfidation at H_2S concentrations as low as 100 ppm. Nonetheless, CaO still appears to be the most reactive. These results are in agreement with the observations of Harrison and Westmoreland (1980) who reported that the most efficient desulfurization occurred at the lowest temperature (about 880°C) at which CaO was first formed from $CaCO_3$.

An increase in the total pressure, with a corresponding increase in the CO_2 and H_2O partial pressures, would inhibit desulfurization by the carbonates (eqs. 5, 7 and 9) but would not affect the equilibria between H_2S and calcium oxide (eqs. 6 and 8). However, at a higher CO_2 partial pressure recarbonation of the oxide competes with sulfidation reaction. Under a 0.4 atmosphere pressure of CO_2, CaO will recarbonate at temperatures below 827°C (Stern and Wiese, 1969). Thus H_2S adsorption by any of the sorbents considered is less efficient at higher pressure. However, most pyrolysis and hydrodesulfurization processes operate at or near atmospheric pressure.

Desulfurization Kinetics

Before any engineering decisions on the effectiveness of oil shale as hydrogen sulfide acceptor are made, detailed information on the thermodynamics and kinetics of reactions involved is required. However, thermodynamics only determine whether a given desulfurization reaction could occur, while the kinetics determine the degree of conversion of a thermodynamically allowable reaction. In particular, kinetic data are essential since in most engineering modeling calculations they are combined with transport equations to predict the performance of a given system.

The intrinsic rate constants for the reactions of calcium carbonate or calcium roxide with H_2S have been reported by a number of investigators. A summary of published work is presented in table 2. The experiments were conducted under conditions where transport effects were minimized. The reported activation energies for the reaction calcium oxide and H_2S range from 3.6 to 38 kcal/mole and those for the carbonate range from 17.3 to 60 kcal/mole. The low values of Westmoreland (1976) and Kamath and Petrie (1981) may be due to diffusion resistances. The activation energy values for the sulfidation of lime as reported by Attar (1978) and Borgwardt et al. (1984) are 37 and 31 kcal/mole. However, the former author believes that the reaction is controlled kinetically while the latter believes that diffusion through the CaS layer is the controlling step. The pre-exponential factors, shown in table 2, also vary by many orders of magnitude. It appears that the data available in the literature are inconclusive. The wide range of reactivities reported in the literature can be attributed either to differences in experimental methodology or in the physical characteristics of minerals employed.

The pore size distribution, porosity, and surface area of the sample as well as the presence of magnesium oxide have been shown to affect the reactivity of calcium minerals with H_2S. The work of Borgwardt et al. (1984) showed that the rate of reaction of lime with H_2S at 700°C is proportional to the 2.3 power of the B.E.T. surface area indicating product layer diffusion control at these conditions. Other authors, however, have observed that the reaction "stops dead" after 5 to 25% conversion due to the solid product layer (Attar, 1979; Squires, 1972). Harvey et al. (1976) concluded that the crystallites of MgO found in hc-dolomite increased the reactivity of the calcium carbonate by maintaining the porosity of the material and hindering the consolidation of the carbonate into larger crystals. Pell (1971) also found that the sulfidation of fc-dolomite particles occurred homogeneously throughout the solid. The inert minerals in oil shale could perform the same function as MgO in dolomite, thereby enhancing the reactivity of the CaO or $CaCO_3$ in oil shale.

The rate of sulfation (reaction with SO_2) of carbonates has also been shown to be highly sample dependent. Borgwardt and Harvey (1972) found the physical properties of the carbonate stones were much more important rate determinants than the composition of the carbonate. Similarly, Fee et al. (1982) found that the chemical composition, pore size distribution, and surface area of each individual limestone or dolomite must be considered before the performance of a solid as an SO_2 acceptor could be predicted. The superior sulfation characteristics of oil shale carbonates over pure dolomite was demonstrated by Fuchs et al. (1978). They observed that the initial rate of sulfation for the hc-dolomite in shale is nearly six times that of pure hc-dolomite under identical experimental conditions. This was attributed to the fine-grained nature of carbonates in oil shale and the high surface area of the devolatilized shale amoung other factors. In the case of sulfidation, as in sulfation, we believe that the reaction kinetics will more likely depend on the physical properties of the solid than on the mineral itself. Therefore only rate measurements made with the oil shale sample will be useful for process design. Published work on the reactivity of the pure minerals is not a reliable substitute.

Since H_2, CO_2, and H_2O are present during hydrotreatment and pyrolysis, their effect on the rate of sulfidation is important. Hydrogen concentrations as low as 3% have lowered the rate of sulfidation of the limestone (Borgwardt and Roache, 1984). The effect increases as the concentration of hydrogen is increased but levels off near 15%. Oddly enough, dolomite is unaffected. The effect of carbon dioxide is important because it is a common component of pyrolysis gas and a product of the sulfidation of carbonates. Ruth (1972) reported that not only the rate of reaction but also the extent of sulfidation of calcium carbonate were greatly increased when raising the CO_2 level of the reactant gas from 3% to 60%. The reaction essentially stopped after 15% conversion when using 3% CO_2 at 600°C whereas complete conversion was achieved at the 60% CO_2 level. At 700°C the effect of the CO_2 level was not particularly significant. The catalytic effect of steam on the rate of sulfidation has also been observed (Pell, 1971; Squires, 1972). Most authors theorize that the gas composition effects the growth and final crystalline structure of the calcium sulfide layer. This in turn enhances or inhibits the rate of hydrogen sulfide, H_2O, or CO_2 diffusion through the solid layer, and changes the overall rate of reaction.

Concluding Remarks

A thorough understanding of the reactions between H_2S and carbonate minerals in oil shale is essential if this material is to be used effectively as an H_2S scavenger. Thermodynamics show that under typical conditions for coal-oil shale pyrolysis, dolomite and calcium oxide are capable of maintaining the desired H_2S concentration in the reactor. Additionally, under typical conditions of char desulfurization, calcium oxide will be an effective sorbent. However, because the gas residence time in an FBR is often on the order of a few seconds, the reaction rates must be high enough for the thermodynamically allowed reactions to reach equilibrium. Therefore, the kinetics of these reactions must be experimentally determined. In addition, a thorough understanding of the influence of the gas environment and the effects of the structural properties of the oil shale particles (raw, retorted, or spent) is essential. We have begun to obtain experimental data for the reactions between H_2S and carbonate minerals in oil shale under typical conditions for pyrolysis and hydrodesulfurization. In the near future, we intend to study the structural changes of oil shale particles during H_2S capture. This information will provide a basis for employing a gas-solid reaction model such as the changing grain size model to predict the behavior of a single oil shale particle during H_2S capture.

References

Attar, A., 1978, Reactions of sulfur in coal-gas reactions, Fuel, Vol. 57, p 209.

Attar, A., and F. Dupius, 1979, The rate and fundamental mechanism of the reaction of hydrogen sulfide with basic minerals in coal, Ind. Eng. Chem. Process Development and Design, Vol. 18, No. 4, p. 607.

Bale, C. W., A. D. Pelton, and W. T. Thompson, 1979, FACT User's Guide, McGill University.

Barin, I., O. Knacke, and O. Kubaschewski, 1977, Thermo-chemical properties of inorganic substances, Springer-Verlag, Berlin.

Borgwardt, R. H. and R. D. Harvey, 1972, Properties of carbonate rocks related to SO_2 reactivity, Environmental Science and Technology, Vol. 6, p. 350-360.

Borgwardt, R. H., N. F. Roache, and K. Bruce, 1984a, Surface area of calcium oxide and kinetics of sulfide formation, Enviromental Progress, Vol. 3, No. 2, p. 129.

Borgwardt, R. H. and N. F. Roache, 1984b, Reaction of H2S and sulfur with limestone particles, Ind. Eng. Chem Process Design Development, Vol. 23, p. 742-748.

Boynton, R. S., 1980, Chemistry and Technology of Lime and Limestone, 2nd ed., John Wiley, Inc.

Burnham, A. K., C. T. Stubblefield, and J. H. Campbell, 1980, Effects of gas environment on mineral reactions in Colorado oil shale, Fuel, Vol. 59, p. 871-877.

Campbell, J. H., 1979, The kinetics of the decomposition of Colorado oil shale II: carbonate minerals, UCRL - 52089.

Chen, C. C., J. K. Floess, L. Fong, J. P. Longwell, and L. B. Evans, 1982, Modeling of an oil shale fluidized bed retorting process using ASPEN, Energy Progress, Vol. 2, No. 3, p. 147-150.

Curran, G. P., C. E. Fink, and E. Gorin, 1967, CO2 Acceptor Gasification Process - studies of acceptor properties, Advances in Chemistry Series, No. 69, American Chemical Society, p. 141-165.

Davidson, M. L., and D. P. Harrison, 1984, Evaluation of the changing grain size model, Eng. Communication, Vol. 25, p. 213-228.

Fee, D. C., K. M. Myles, W. I. Wilson, L. S. Fan, G. W. Smith, S. H. Wong, J. A. Shearer, J. F. Lenc, and I. Johnson, 1980, Sulfur control in fluidized bed combustors; methodology for predicting the performance of limestone and dolomite sorbents, Report to DOE, ANL/FE-80-10.

Harvey, R. D., G. Kan, R. A. Graff, and A. M. Squires, 1976, Behavior of dolomite in absorption of H2S from fuel gas, ISGS Reprint Series, 1977C.

Haul and Markus, 1952, J. Appl. Chemistry, Vol. 2, p. 298.

Hill, K. J., and E. K. Winters, 1956, Thermal dissociation pressure of calcium carbonate, J. Phys. Chem., Vol. 60, p. 1361-1362.

Huang, E. T. and A. H. Pulsifer, 1979, Coal desulfurization during gaseous treatment, ACS Symposium Series, No. 64, American Chemical Society, p. 290-304.

Jones, J. F., M. R. Schmid, M. E. Sacks, Y. C. Chen, C. A. Gray, R. T. Eddinger, 1966, COED final report, Jan.-Oct. 1966, OCR, Department of Interior.

Kamath, V. S. and T. W. Petrie, 1981, Rate of reaction of hydrogen sulfide - carbonyl sulfide mixtures with fully calcined dolomite, SIU Carbondale, Environmental Science and Technology, Vol. 15, No. 8, p. 966.

MacIntire, W., and T. Stansell, 1953, Ind. and Eng. Chemistry, Vol. 45, p. 1548.

McCarthy, D. J. and H. J. Poynton, 1984, Formation of calcium silicates during processing of Julia Creek oil shale, Fuel, Vol. 63, p. 769.

Mills, K. C., 1974, Thermodynamic data for inorganic sulfides, selenides and tellurides, Butterworths Inc., London.

Pell, M., 1971, Reaction of hydrogen sulfide with fully calcined dolomite, PhD thesis, City University of New York.

Robinson, L., 1976, Hydrodesulfurization of char, Fuel, Vol. 55, p. 193-201.

Rosenqvist, T., 1951, A thermodynamic study of the reaction CaS + H_2 H_2S + CaO and the desulfurization of liquid metals with lime, J. Metals Trans., Vol. 3, p. 535-40.

Ruth, L. A., A. M. Squires, R. A. Graff, Desulfurization of fuels with half-calcined dolomite: first kinetic data, Environmental Science and Technology, Vol. 6, No. 12, p. 1009.

Schmalfeld, P., 1975, The use of the Lurgi-Rhurgas process for the distillation of oil shale, Quart Colorado School of Mines, Vol. 670, No. 3, p. 129-145.

Sitnai, O., 1984, Process concept for retorting of Julia Creek oil shale, Energy Progress, Vol. 4, No. 2, p. 100-104.

Steen, C. L., K. Li, and F. Rogan, 1980, Half-calcination of dolomite at high pressures. Kinetics and structural changes, Environmental Science and Technology, Vol. 14, No. 5, p. 588.

Stern, K. H. and E. L. Wiese, 1969, High temperature properties and decomposition of inorganic salts, part 2: carbonates, NSRDS - NBS30, p. 19.

Squires, A. M., 1972, New systems for clean power, Int. J. Sulfur Chemistry, Pt B, Vol. 7, No. 1, p. 85.

Uno, T., 1951, Tetsu To Hagana (Iron and Steel) Vol. 37, p. 14-17.

Weiss, H., 1982, Retorting of oil shale - background, status, and potential of the Lurgi-Ruhrgas process, ACS symposium, Oil shale retorting - Latest developments, March 28 - April 12, Las Vegas, Nevada.

Westmoreland, P. R., J. B. Gibson, D. P. Harrison, Comparative kinetics of high-temperature reaction between H_2S and selected metal oxides, Environmental Science and Technology, Vol. 11, No. 5, p. 488.

Westmoreland, P. R. and D. P. Harrison, 1976, Evaluation of candidate solids for high-temperature desulfurization of low-Btu gases, Environimental Science and Technology, Vol. 10, No. 7, p. 659.

Zielke, C. W., G. P. Curran and G. E. Gorning, 1954, Desulfurization of low temperature char by partial gasification, Ind. Eng. Chem., Vol. 46, No. 1, p. 53-56.

Table 2. Experimental Techniques and Results of Kinetic Studies, Part I

Reference	Kinetic Expression (Temperature range)	Reactor	K_o	E_a(kcal/mole)
Attar (1978)	Rate = K[Solid][H_2S] (400-800°C)	Pulsed Differential Reactor, Packed bed design	-	$CaCO_3$ 17.3 CaO 37.0 $CaCO_3MgCO_3$ 18.9
Borgwardt (1984a)	Rate = K[CaO][H_2S] (600-900°C)	Differential Reactor, Packed bed design	1.2×10^8 L·cm/mole H_2S·min [a]	37
Borgwardt (1984b)	Rate = $\frac{K}{Dp}$ [$CaCO_3$][H_2S] (550-850°C)	Differential Reactor, Packed bed design	8×10^8 L·cm/mole H_2S·min [a] at Dp = 2.8um	42.6
Davidson (1984)	Rate = AK[H_2S]; where A = Wt% CaO (625-950°C)	Thermobalance	8.25×10^4 L·cm/mole H_2S·min [b]	27
Kamath (1981)	Rate = K[CaO] (600-800°C)	Thermobalance	$K_{600} = 1.1 \times 10^{-4}[H2S]^{0.76}$ sec^{-1} $K_{700} = 1.43 \times 10^{-4}[H2S]^{1.01}$ sec^{-1} $K_{800} = 1.61 \times 10^{-4}[H2S]^{1.22}$ sec^{-1}	
Pell (1971)	Rate = AK[H_2S]; where A = Wt% CaO (700-900°C)	Thermobalance	4.96×10^5 L/mole H_2S·min	22.9
Ruth (1972)	Rate = K'[$CaCO_3$] (550-800°C)	Modified Dupont TGA	-	60
Westmoreland (1977)	Rate = K'[CaO][H_2S]^N (300-800°C)	Thermobalance	0.038 L·cm/min·mgmole	N = 1 5.16

[a] Estimate from data given

[b] A recalculation of Pell's data

Table 2. Experimental Techniques and Results of Kinetic Studies, Part II

Reference	Material	Material Properties	Gas Composition & Flow Properties
Attar (1973)	Calcite, Lime, and Dolomite	-200 mesh, 0.1-0.5g sample	H_2S pulse = 1 x 10^{-6} mole/pulse in steady stream of He, flow rate not given but assumed to be low because gas diffusion was controlling at times
Borgwardt (1984a)	CaO from Calcined Limestone	2um limestone calcined at 700°C for 90 sec, 15 mg sample, surface area = 5.8 m^2/g, BCR 2061	5000 ppm H_2S, 70% CO_2, balance N_2
Borgwardt (1984b)	Limestone	Fredonia Valley White, Fredonia, KY, ratio Ca/Mg = 73/1, BC 2061 1-10 um limestone particles dispersed in quartz wool	5000 ppm H_2S, 70% CO_2, balance N_2, 5 L/min at 25°C, 490 cm^2/s at 750°C, gas diffusion was not a problem at this rate, exposure time = 30-55 min
Davidson (1984)	Fully-calcined Dolomite	surface area = 14 m^2/g, 124-380 mg samples, sphere diameter = 0.277 to 0.406 cm	5% H_2S, 7.5% H_2
Kamath (1981)	Fully-calcined Dolomite	-30+50 mesh, Dp = 400um, Pfizer Corp., Gibsonville, Ohio, ratio Ca/Mg = 0.84	0.5-5% H_2S, 20% H_2, 30% CO, balance N_2, 500 SCCM used, no difference at 1000 SCCM
Pell (1971)	Fully-calcined Dolomite	-80+325 mesh, ratio Ca/Mg = 1.09	0.5-20% H_2S, 7.5% H_2, balance N_2, H_2O used at times, flowrate = 0.5 L/min (STP), Reynolds number = 1
Ruth (1972)	Half-calcined Dolomite	Greenfield formation, 25mg sample, -250+270 mesh, dolomite calcined immediately before reaction in TGA, BCR 1337 and 1930	0.5-20% H_2S, various levels of CO_2, H_2, and N_2, flow rate = 100-300 mL/min
Westmoreland (1977)	Pure CaO	100 mesh heated to 500°C in an inert gas, surface area = 17.3 m^2/g	1.9-7% H_2S, ratio H_2/H_2S = 5:1, balance N_2, volumetric flowrate set to eliminate external mass transfer resistance

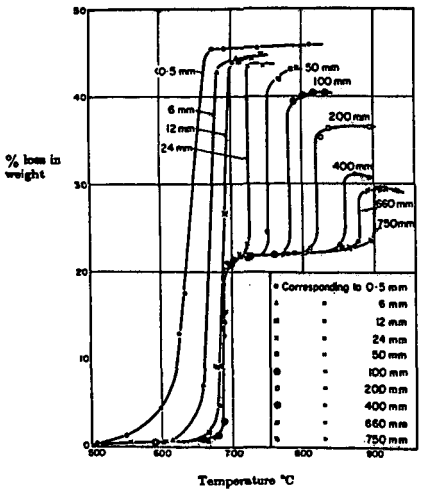

Figure 1. The thermogravimetric analysis of dolomite at various temperatures and CO_2 pressures.

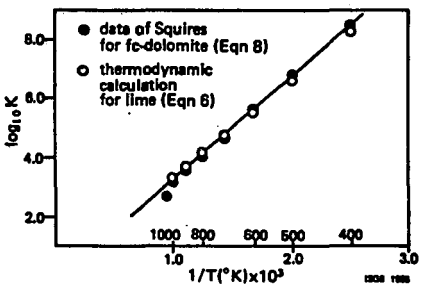

Figure 2. Log K_{eq} vs 1/T for the adsorption of H_2S by CaO.

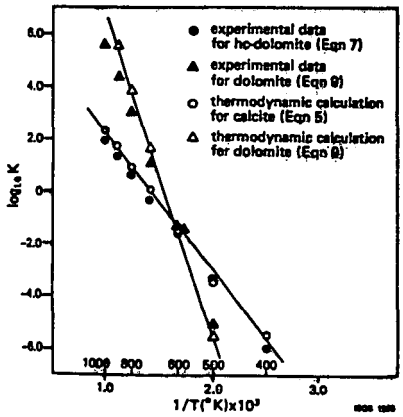

Figure 3. LogK_{eq} vs 1/T for the adsorption of H_2S by various forms of $CaCO_3$.

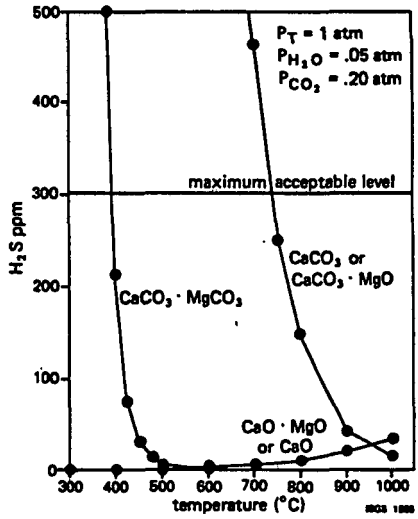

Figure 4. Equilibrium partial pressure of H_2S in the presence of oil shale minerals.

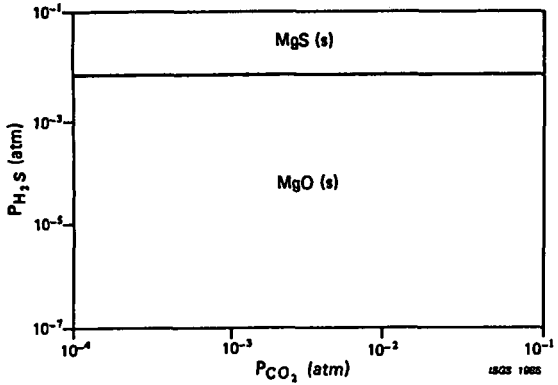

Figure 5. Phase stability diagram for the Mg-H-O-S-C system, T=1227°C, P_{H_2O} = 0.05 atm.

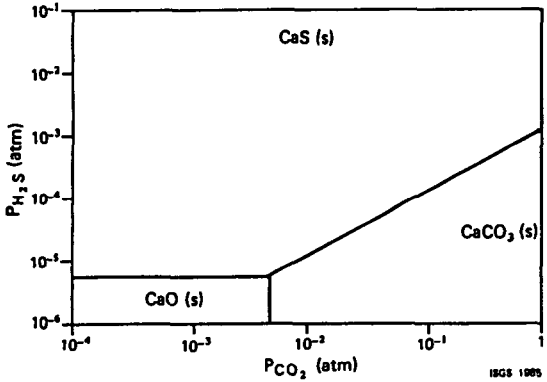

Figure 6. Phase stability diagram for the Ca-H-O-S-C system, T=600°C, P_{H_2O} = 0.05 atm.

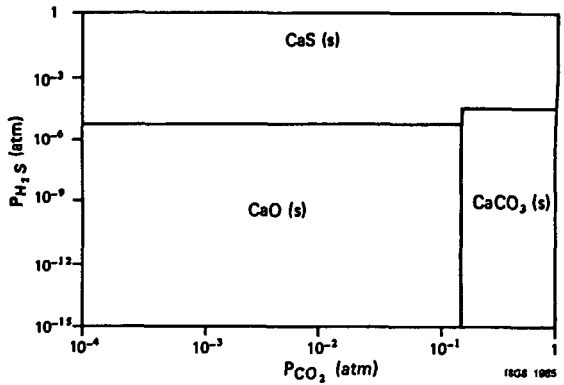

Figure 7. Phase stability diagram for the Ca-H-O-S-C system, T=750°C, P_{H_2O} = 0.05 atm.